Amyloid
The Journal of Protein Folding Disorders
http://informahealthcare.com/amy
ISSN: 1350-6129 (print), 1744-2818 (electronic)
Amyloid, 2016; 23(2): 109–118
 DOI: 10.3109/13506129.2016.1160882

Taylor & Francis
Taylor & Francis Group

ORIGINAL ARTICLE

Preclinical evaluation of RNAi as a treatment for transthyretin-mediated amyloidosis

James S. Butler[1], Amy Chan[1]*, Susete Costelha[2,3]*, Shannon Fishman[1]*, Jennifer L. S. Willoughby[1]*, Todd D. Borland[1]*, Stuart Milstein[1], Donald J. Foster[1], Paula Gonçalves[2,3], Qingmin Chen[1], June Qin[1], Brian R. Bettencourt[1], Dinah W. Sah[1], Rene Alvarez[1], Kallanthottathil G. Rajeev[1], Muthiah Manoharan[1], Kevin Fitzgerald[1], Rachel E. Meyers[1], Saraswathy V. Nochur[1], Maria J. Saraiva[2,3], and Tracy S. Zimmermann[1]

[1]*Alnylam Pharmaceuticals, Cambridge, MA, USA,* [2]*Instituto de Investigação e Inovação em Saúde, Universidade do Porto, Porto, Portugal,* [3]*Molecular Neurobiology, IBMC – Institute for Molecular and Cell Biology Porto, Porto, Portugal*

Abstract

ATTR amyloidosis is a systemic, debilitating and fatal disease caused by transthyretin (TTR) amyloid accumulation. RNA interference (RNAi) is a clinically validated technology that may be a promising approach to the treatment of ATTR amyloidosis. The vast majority of TTR, the soluble precursor of TTR amyloid, is expressed and synthesized in the liver. RNAi technology enables robust hepatic gene silencing, the goal of which would be to reduce systemic levels of TTR and mitigate many of the clinical manifestations of ATTR that arise from hepatic TTR expression. To test this hypothesis, TTR-targeting siRNAs were evaluated in a murine model of hereditary ATTR amyloidosis. RNAi-mediated silencing of hepatic TTR expression inhibited TTR deposition and facilitated regression of existing TTR deposits in pathologically relevant tissues. Further, the extent of deposit regression correlated with the level of RNAi-mediated knockdown. In comparison to the TTR stabilizer, tafamidis, RNAi-mediated TTR knockdown led to greater regression of TTR deposits across a broader range of affected tissues. Together, the data presented herein support the therapeutic hypothesis behind TTR lowering and highlight the potential of RNAi in the treatment of patients afflicted with ATTR amyloidosis.

Abbreviations: ATTR amyloidosis: transthyretin mediated amyloidosis; GalNAc: *N*-acetylgalactosamine; h-ATTR: hereditary ATTR; LNP: lipid nanoparticle; PD: pharmacodynamics; RNAi: RNA interference; siRNA: small interfering RNA; TTR: transthyretin; wt: wild-type

Keywords

GalNAc, gene silencing, lipid nanoparticle, siRNA, therapeutic

History

Received 12 November 2015
Revised 21 February 2016
Accepted 29 February 2016
Published online 31 March 2016

Introduction

Transthyretin (TTR) is a 127 amino acid, 55-kDa homotetrameric serum transport protein that is primarily expressed in the liver [1–3]. Its primary function is to transport Vitamin A (retinol) through its interaction with the retinol binding protein [4]. The TTR tetramer also contains two hydrophobic binding pockets which bind the thyroid hormone thyroxine (T4), although in humans it serves a minor role in this capacity [5,6]. Although the majority of newly synthesized TTR protein folds and functions properly, TTR protein misfolding can occur [7]. TTR misfolding is exacerbated by destabilizing mutation and proteolysis and, if left uncorrected, misfolded TTR has a propensity to form pathologic amyloid fibrils [8–11]. TTR-mediated amyloidosis (ATTR amyloidosis) is a progressive, systemic and ultimately fatal disease resulting from the damage caused by the extrahepatic deposition of insoluble TTR fibrils [12–14]. TTR-containing amyloid fibrils can deposit in peripheral and central nervous systems, the gastrointestinal tract, eye, kidney and/or the heart. ATTR amyloidosis can be broadly classified based on TTR genotype: hereditary ATTR amyloidosis if a mutant allele is present and wild-type ATTR if a mutant allele is absent [15]. The pattern of amyloid deposition and age of disease onset are dictated to a large degree by which TTR allele is expressed, although other unidentified factors modify clinical presentation and disease penetrance [16–19]. Manifestation of the hereditary ATTR amyloidosis disease phenotype is somewhat heterogeneous and is a direct result of the specific amyloidogenic mutation. To date, over 100 such mutations have been characterized (http://amyloidosismutations.com) [20]. Clinical manifestation can include sensory and motor neuropathy, autonomic neuropathy, various ocular sequelae, nephropathy, cerebral angiopathy and/or cardiomyopathy [19]. In contrast to hereditary ATTR amyloidosis, wild-type ATTR amyloidosis results from the misfolding of

*These authors contributed equally to this work.

Address for correspondence: James S. Butler, Alnylam Pharmaceuticals, Cambridge, MA 02142, USA. Tel: +1 617 551 8200. E-mail: jbutler@alnylam.com

wt TTR protein with deposition occurring predominantly in the heart [13,21]. Clinical presentation of wild-type ATTR amyloidosis, which includes carpal tunnel syndrome and cardiomyopathy, typically occurs much later in life relative to the hereditary forms, and likely reflects the fact that wt TTR is less prone to misfolding than other amyloidogenic variants.

Although disease manifestation varies across the different forms of ATTR amyloidosis, the common feature of these diseases is the misfolding of TTR protein that ultimately results in amyloid formation and deposition. As such, mitigation of TTR amyloid deposition is crucial to the development of any successful therapeutic treatment for all forms of ATTR amyloidosis. Orthotopic liver transplantation has been used to effectively slow the progression of hereditary ATTR amyloidosis with polyneuropathy by eliminating mutant TTR synthesis and, in some cases, resulted in clinical improvement [22,23]. However, in addition to the associated complications of liver transplantation, this approach appears to be limited to sub-populations of hereditary ATTR amyloidosis with polyneuropathy. In other ATTR amyloidosis subtypes, established deposits appear to recruit misfolded wt TTR leading to continued disease progression, suggesting elimination of mutant TTR alone is insufficient for disease modification [24]. Tetramer stabilizers are a class of small molecule therapies currently under development and even approved in certain geographic locales for the treatment of ATTR amyloidosis. These modalities aim to limit TTR aggregation by binding and stabilizing the properly folded tetramer, thereby decreasing the concentration of aggregation-prone species [25]. This approach is based on the observation that a naturally occurring TTR variant, Thr119Met (p.Thr139Met), essentially nullifies the deleterious effects of the Val30Met mutation when presented as a compound heterozygote by stabilizing the mixed TTR tetramer [26,27]. To date, data from clinical trials evaluating the TTR tetramer stabilizers tafamidis and diflunisal suggest that this approach can slow the rate of ATTR amyloidosis progression [28,29], although they do not appear to afford the same level of protection offered by the Thr119Met suppressor mutation. At present, it is unclear if this is due to the relatively late introduction of pharmacologic intervention, relative to the life-long protection of the innate Thr119Met mutation, or due to the different mechanisms of stabilization [25,30]. Regardless, there is still a need for effective treatments for ATTR amyloidosis.

RNA interference (RNAi) is a naturally occurring biological process by which small interfering RNA (siRNA) can direct sequence-specific degradation of mRNA, leading to inhibition of synthesis of the corresponding protein [31,32]. The ability to selectively suppress disease-causing genes via RNAi has emerged as a novel and highly promising therapeutic approach for the treatment of genetic, metabolic, infectious and malignant diseases, with several clinical programs in development [33,34]. Recent advances in the ability to use lipid nanoparticles and *N*-acetylgalactosamine (GalNAc)-siRNA conjugates for efficient and specific delivery of siRNA to the liver have paved the way for development of RNAi-based therapeutics for disease targets expressed in the liver [35–39]. As such, an RNAi therapeutic strategy is well-suited to the treatment of ATTR amyloidosis. Specifically, the therapeutic hypothesis behind this strategy predicts that silencing TTR gene expression will reduce the total amount of TTR protein, both folded and misfolded, that becomes a substrate for amyloid fiber formation, thereby reducing tissue burden and the consequences thereof. Given the vast majority of pathogenic protein in ATTR amyloidosis originates in the liver [2], liver specific gene silencing enabled by current delivery technologies should result in nearly complete reduction of systemic TTR levels. Finally, given the ability to silence all known disease causing TTR variants, including wt, an RNAi therapy may be not only an effective approach for the treatment of ATTR amyloidosis but also more generally applicable.

In this report we describe preclinical data that supports the therapeutic hypothesis that RNAi-mediated depletion of the disease-causing TTR protein could lead to reduced TTR aggregation/deposition and thereby support the use of RNAi as a promising approach for the treatment of ATTR amyloidosis.

Methods

siRNA formulations

TTR specific siRNAs (siTTR) target a conserved region in the 3′-untranslated region (3′-UTR) of human TTR and have been described elsewhere [40]; a non-targeting siRNA (siCTRL) was used as a negative control [41]. siTTR1 and siCTRL1 are intravenously administered siRNA formulations that employ a DLin-MC3-DMA-based lipid nanoparticle (LNP) delivery system [39,42]. siTTR2 is a subcutaneously administered siRNA formulation that employ an *N*-acetylgalactosamine (GalNAc) conjugate delivery platform [35]. Patisiran, previously called ALN-TTR02, is a DLin-MC3-DMA-based LNP siRNA formulation [36]. Revusiran, previously called ALN-TTRsc, is an siRNA-GalNAc conjugate [43]. Although not explicitly evaluated in these studies, the PK properties of similar compounds have been described previously [35,36,44,45].

In vitro TTR gene knockdown

Dual-Luciferase (Dual-Luc) reporter constructs were created for each mutant human TTR gene to evaluate *in vitro* knockdown efficacy. To create Dual-Luc reporter constructs, site directed mutagenesis was performed on a cDNA clone containing the sequence found in NM_000371.2 using the Quikchange II Site directed mutagenesis kit (Agilent, Santa Clara, CA). Mutations were subcloned into psiCHECK2 Dual-Luc vector (Promega, Madison, WI) at the NotI restriction site and sequenced to confirm the presence of the mutation and orientation of the insert. Cos7 cells were transfected with plasmids that express wt or mutant full-length TTR cDNA sequences fused to the 3′ end of the luciferase gene. Approximately 24 h after transfection of plasmid, siTTR was transfected by using lipofectamine RNAiMax (Invitrogen, Waltham, MA) following the manufacturer's protocol. Twenty-four hours after transfection of siTTR, luciferase was measured. A Dual-Luc construct lacking the TTR insertion (Empty Vector) was included as a negative control. Data were expressed as TTR levels relative to cells treated with the non-targeting control siCTRL.

In vivo biomarker analysis

Hepatic TTR and GAPDH mRNA were quantified using the branched DNA assay using species-specific probes (QuantiGene Reagent System, Panomics, Fremont, CA). For each animal, TTR mRNA data are normalized first to GAPDH mRNA. The TTR/GAPDH ratio is further normalized to the mean TTR/GAPDH ratio of control treated animals to calculate the relative TTR mRNA concentration.

Serum TTR protein was measured using a validated TTR enzyme-linked immunosorbent assay (ELISA) as previously described [36]. A human TTR protein standard (Sigma–Aldrich, P1742, St. Louis, MO) was employed for hTTR V30M HSF1$^{\pm}$ mouse serum analysis. Purified TTR from the serum of *Macaca fascicularis* was employed in the analysis of monkey serum. Serum TTR protein concentrations are normalized to pre-dose baseline serum TTR and expressed as relative serum TTR protein concentration. Where pre-dose baseline measurements are unavailable, the serum TTR is normalized to the serum concentration of control treated animals instead (see figure legends).

Evaluation of siTTR1 and siTTR2 in hTTR V30M HSF1$^{\pm}$ mice

In vivo experiments using hTTR V30M HSF1$^{\pm}$ mice were conducted at University of Porto, Portugal (Saraiva Lab) and in accordance with the European Communities Council Directive 2010/63/EU. The hTTR V30M HSF1$^{\pm}$ mouse model has been described previously [46]. siTTR1 or siCTRL1 were administered via a bolus tail vein injection (10 µl/g dose volume). siTTR2 or PBS were administered via subcutaneous injection (10 µl/g dose volume). Gross observation indicated no changes in animal behavior or health throughout the course of the experiment. Hepatic TTR mRNA and serum TTR protein levels were evaluated as described earlier. TTR tissue deposition was evaluated by immunohistochemical tissue analyses, quantified as previously described [46], and normalized to the mean TTR tissue deposition of control treated animals, respectively. Specific study designs are described below.

Correlation analysis of TTR regression and serum TTR protein in hTTR V30M HSF1$^{\pm}$ mice

hTTR V30M HSF1$^{\pm}$ mice received subcutaneous administration of siTTR2 once weekly for 12 weeks at dose levels of 1, 2.5 and 25 mg/kg. Mice were sacrificed 2 days after the 12th and final dose and evaluated for TTR tissue deposition as described earlier. To evaluate the correlation of TTR knockdown and the regression of TTR tissue deposits, the total exposure to serum TTR was calculated. To calculate exposure, serum concentrations were measured once every week beginning prior to the first dose and continuing throughout the study (data not shown). From this, serum TTR exposure, or area under the curve (AUC), was calculated using the trapezoidal method for AUC. To calculate mean relative serum TTR concentration over the course of the experiment, the mean absolute serum TTR concentration for each animal was calculated by dividing the AUC by the total time interval. This number was then normalized to the group mean serum TTR concentration of PBS treated animals. Both relative knockdown and exposure (AUC) for each animal are plotted in Figure 4(A).

Evaluation of tafamidis in hTTR V30M HSF1$^{\pm}$ mice

Tafamidis/meglumine (tafamidis) and its respective meglumine only control (meglumine) were prepared as previously described [47]. Four hundred microliters of 2 mg/ml tafamidis (0.8 mg total) or its respective meglumine control were administered via subcutaneous injection to 15-month-old hTTR V30M HSF1$^{\pm}$ mice on days 0, 3, 5, 7, 10, 12, 14, 17, 19, 21, 24, 26, 28, 31, 33, 35 and 38. TTR tissue deposition was evaluated on day 52 as described earlier. To confirm tafamidis-mediated stabilization of serum TTR, serum TTR tetramer stability was analyzed on days -7, 9, 23 and 37 using a modified version of a previously described TTR tetramer stability assay [8]. See Supplementary Figure 2 for more detail on assay conditions and tetramer detection and quantitation. To quantify the extent of stabilization, % TTR tetramer stabilization was calculated using the following equation as previously described [48]:

$$\frac{\left(\begin{array}{l}\text{Fraction TTR Tetramer (dosed)}\\ -\text{ Fraction TTR Tetramer (pre-dose)}\end{array}\right)}{\text{Fraction TTR tetramer (pre-dose)}} \times 100$$

Non-human primate studies

All non-human primate studies were conducted at Charles River Laboratories in experimentally naive male or female Chinese cynomolgus monkeys (*Macaca fascicularis*) between 2 and 4 years of age and between 2 and 4 kg in body weight. Animals were housed in accordance with the USDA Animal Welfare Act (9 CFR, Parts 1, 2 and 3) and as described in the Guide for the Care and Use of Laboratory Animals. For animals receiving patisiran, dosing material was administered using 60-min intravenous infusion at a dose volume of 20 ml/kg via the saphenous vein. For animals receiving revusiran, dosing material was administered at a dose volume of 1.5 ml/kg as a series of subcutaneous doses, divided into two or three dose sites of $\geq$1.2 ml and $\leq$2 ml per injection site, into the scapular and mid-dorsal regions. Where applicable, a non-targeting siRNA (siCTRL) or phosphate buffered saline (PBS) served as the control article and was administered at a dose volume equal to the respective test article volume. Gross observation indicated no changes in animal behavior or health throughout the course of the experiment. Serum was collected at specified study time points for downstream pharmacodynamic analyzes.

Statistical analyses

All curve fitting and statistical analyses were performed using GraphPad Prism (v. 6.02, La Jolla, CA). The specific statistical analysis for each experiment is listed in the respective figure legend.

Results

siTTR silences wt and mutant TTR variants with similar efficacy and potency

The RNAi therapeutic candidates currently in the clinic and those used in pre-clinical studies described in this report

target a conserved region in the 3′-UTR of the TTR gene that does not overlap with any of the documented TTR variants [40]. As such, it is expected that all TTR variants as well as wt TTR should be inhibited with similar efficacy and potency. To experimentally validate this hypothesis, a series of Dual-Luciferase (Dual-Luc) *in vitro* gene expression constructs were developed to evaluate the impact of mutation on siTTR activity. The Dual-Luc reporter assay construct contained the full-length TTR cDNA sequence fused to the 3′ end of the *Renilla* luciferase gene, thereby making this hybrid gene construct sensitive to siTTR treatment. To evaluate the impact of mutation relative to wt TTR, single nucleotide polymorphisms (SNPs) associated with some of the more prevalent ATTR variants were introduced into each respective vector. As shown in Figure 1, siTTR silenced wt and mutant TTR gene constructs with similar efficacy and potency, suggesting wt and mutant TTR variants will be similarly silenced in ATTR amyloidosis patients.

siTTR formulations knockdown TTR gene expression *in vivo*

Two different siRNA formulations targeting TTR are currently being evaluated in human clinical studies. One of these formulations, siTTR1, employs a lipid nanoparticle (LNP) delivery platform [36] while the other formulation, siTTR2, employs an *N*-acetylgalactosamine (GalNAc) ligand to facilitate siRNA delivery to hepatocytes [35]. Although these formulations employ different mechanisms of siRNA delivery to hepatocytes, they are identical with respect to their end goal of silencing hepatic TTR gene expression for therapeutic benefit.

To determine whether these siRNA formulations can mediate *in vivo* TTR gene silencing, siRNA formulations targeting TTR were administered to hTTR V30M HSF1$^{\pm}$ mice, a transgenic mouse line which expresses the pathogenic human Val30Met (p.Val50Met) TTR variant [46]. hTTR V30M HSF1$^{\pm}$ transgenic mice were administered a single injection of siTTR1, siTTR2 or their respective controls and evaluated for liver TTR mRNA and serum TTR protein knockdown 48 h after administration. Single dose administration of siTTR1 led to >85% knockdown of hepatic TTR mRNA and serum TTR protein (Figure 2A). Similarly, administration of siTTR2 led to >70% knockdown of TTR mRNA and serum TTR (Figure 2B). Together, the data confirm that both delivery modalities effectively silence TTR gene expression *in vivo*.

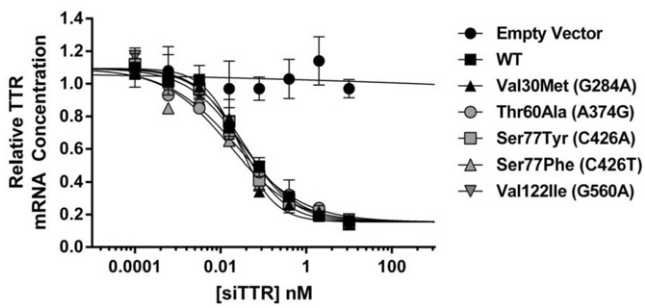

Figure 1. siTTR silences Wild-type (WT) and mutant TTR variants with similar potency. *In vitro* analysis of siRNAs targeting TTR using a Dual-Luciferase (Dual-Luc) reporter assay. For each variant, the corresponding nucleic acid change is listed in parentheses in the symbol legend. Data are expressed as normalized mRNA expression; error bars represent SEM ($n = 2$). Data fitted to a 4-parameter logistic non-linear regression; fitted EC_{50} values are 36, 28, 23, 30, 16 and 33 pM for WT, Val30Met (p.Val50Met), Thr60Ala (p.Thr80Ala), Ser77Tyr (p.Ser97Tyr), Ser77Phe (p.Ser97Phe) and Val122Ile (p.Val142Ile) variants, respectively.

siTTR formulations prevent mutant TTR protein deposition in a mouse model of ATTR amyloidosis

hTTR V30M HSF1$^{\pm}$ transgenic mice do not express endogenous murine TTR, which is known to stabilize human mutant TTR tetramers [49]. Further, one copy of endogenous heat shock factor 1 (HSF-1) is inactivated resulting in mice with compromised HSF-1 activity [50]. As a consequence of these genetic modifications, these mice exhibit non-fibrillar TTR protein deposition in organs consistent with the pattern observed in patients with ATTR Val30Met. The phenotype is fully penetrant in mice older than 12 months of age and is therefore a good model for evaluating the therapeutic hypothesis of TTR lowering in ATTR amyloidosis [46].

To evaluate the impact of TTR silencing on regression of existing TTR deposits, 15-month-old hTTR V30M HSF1$^{\pm}$ mice were intravenously administered siTTR1 or its respective control (siCTRL1) at 1 mg/kg once every 2 weeks for a total of four doses (days 0, 14, 28 and 42). Serum TTR protein levels and TTR protein tissue deposition were evaluated 1 week after the fourth and final dose (day 49). At 15 months

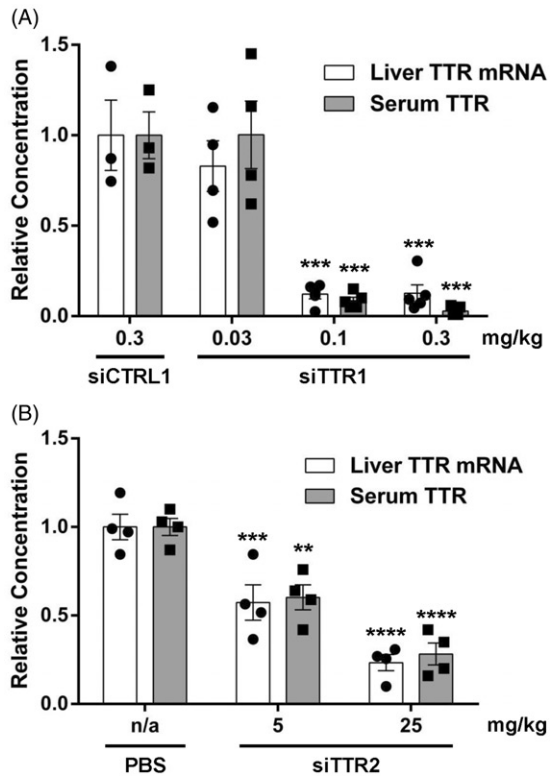

Figure 2. RNAi-mediated knockdown of hepatic TTR gene expression. Liver TTR mRNA and serum TTR protein following single dose administration of siTTR1 or siCTRL1 (A) or siTTR2 or PBS (B) in hTTR V30M HSF1$^{\pm}$ mice. Bar height represents group mean concentration; error bar represents the SEM; individual data point for each animal displayed as symbols within the bar. Treatment effect evaluated using 2-way ANOVA with Bonferroni's multiple comparison test (**$p < 0.01$, ***$p < 0.001$, ****$p < 0.0001$). In panel (A), $n = 3$ for siCTRL1, $n = 5$ for all other groups. In panel (B), $n = 4$ for all groups.

of age, the TTR deposition phenotype is fully penetrant and as such all mice would be expected to begin the experiment with extensive tissue deposition. Administration of siTTR1 resulted in robust (>95%) and sustained knockdown of serum TTR protein relative to control (Figure 3A). TTR deposition was evaluated by immunohistochemical staining and quantified in tissues associated with ATTR Val30Met as previously described [46]. In contrast to control treated animals, repeat administration of siTTR1 resulted in a reduction of TTR immunoreactivity in the esophagus, stomach, duodenum, colon, sciatic nerve and dorsal root ganglion (Figure 3B). Quantitation of immunoreactivity demonstrated that siTTR1 treated mice exhibited robust (70–80%) and statistically significant reduction of TTR deposits in the esophagus, duodenum, colon, sciatic nerve and dorsal root ganglion, with some animals achieving nearly complete TTR deposit reduction (Figure 3C). TTR lowering failed to elicit a statistically significant reduction in TTR deposition in the stomach, likely due to the greater variability observed in this tissue and treatment group. However, the majority of animals exhibited robust (60–90%) TTR deposit reduction and suggests that, while not statistically significant, the effect of TTR lowering on stomach deposition is likely real. Although primarily expressed in the liver, TTR is also expressed at low levels in other tissues including the choroid plexus, retinal epithelium of the eye and the alpha islets of the pancreas [51–53]. Consistent with liver-specific delivery of siTTR1, reduction of TTR synthesis in these tissues was not observed (Figure 3B). Similarly, weekly subcutaneous administration of siTTR2 at 25 mg/kg (see below) resulted in >95% knockdown of serum TTR and in statistically significant reductions of TTR deposition in all tissues examined (Figure 4A and B). Also similar to siTTR1, reduction in the choroid plexus, retinal epithelium of the eye and the alpha islets of the pancreas was not observed upon repeat administration of siTTR2, consistent with the liver specific delivery of GalNAc-conjugated siRNAs (data not shown). Together, the data suggest that regardless of the delivery modality, RNAi-mediated knockdown of liver derived TTR was sufficient to inhibit the deposition and facilitate the regression of TTR

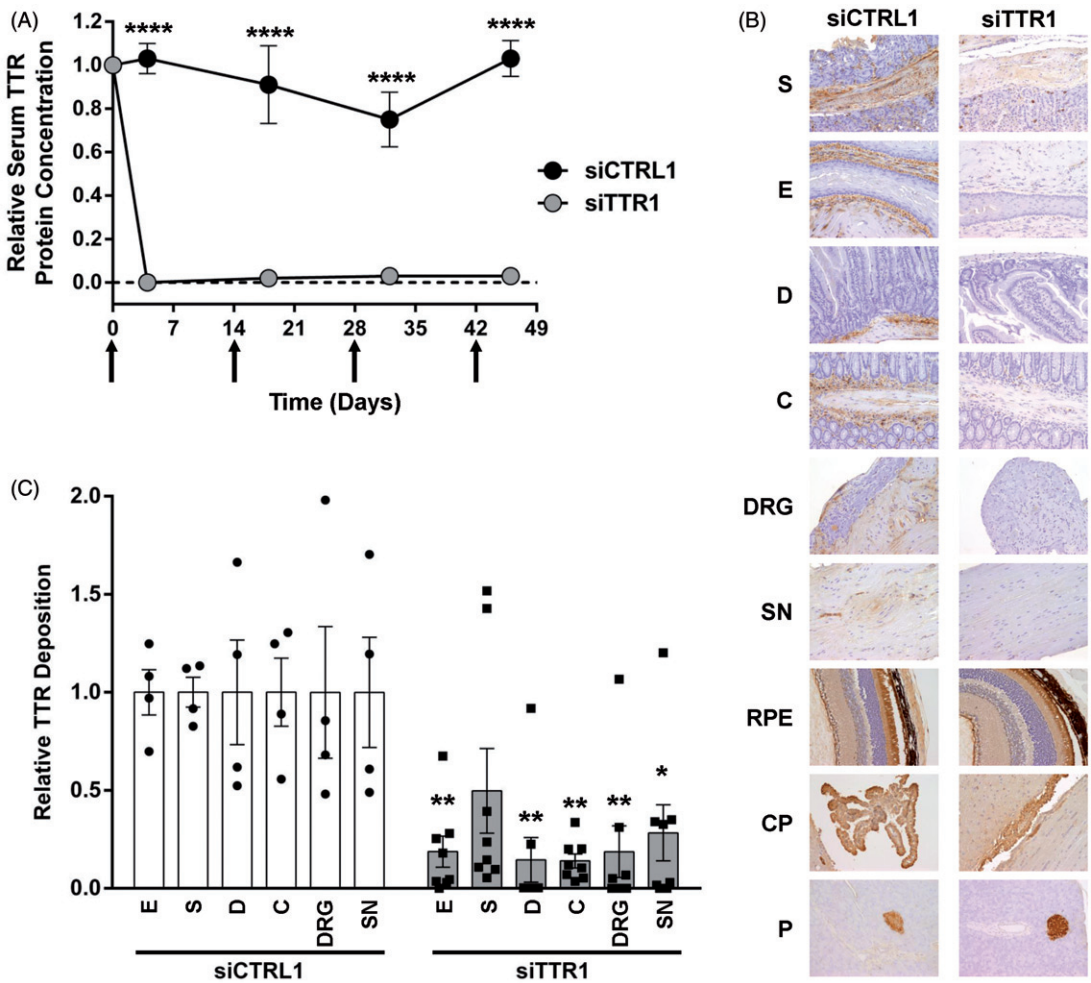

Figure 3. RNAi-mediated TTR knockdown prevents TTR deposition in hTTR V30M HSF1$^{\pm}$ mice. TTR tissue deposition in 15-month-old hTTR V30M HSF1$^{\pm}$ mice following repeat administration of siTTR1 or siCTRL1. (A) Relative serum TTR protein knockdown. (B) Representative images of immunohistochemical (IHC) TTR protein detection in: E, esophagus; S, stomach; D, duodenum; C, colon; SN, sciatic nerve; DRG, dorsal root ganglion; RPE, retinal pigmentosa epithelium; CP, choroid plexus; P, pancreatic alpha cells. (C) Relative TTR tissue deposition in select tissues. Tissue abbreviations as described earlier. In panel (A), symbols represent group mean relative concentration; error bars represent the SEM; arrows indicate administration of siTTR1 or siCTRL1. In panel (C), bar height represents group mean; error bar represents the SEM; individual data point for each animal displayed as symbols within the bar. The treatment effect in (A) and (C) was determined using 2-way ANOVA with Bonferroni's multiple comparison test relative to respective control (*$p<0.05$, **$p<0.01$, ****$p<0.0001$). siCTRL, $n=4$; siTTR1, $n=8$.

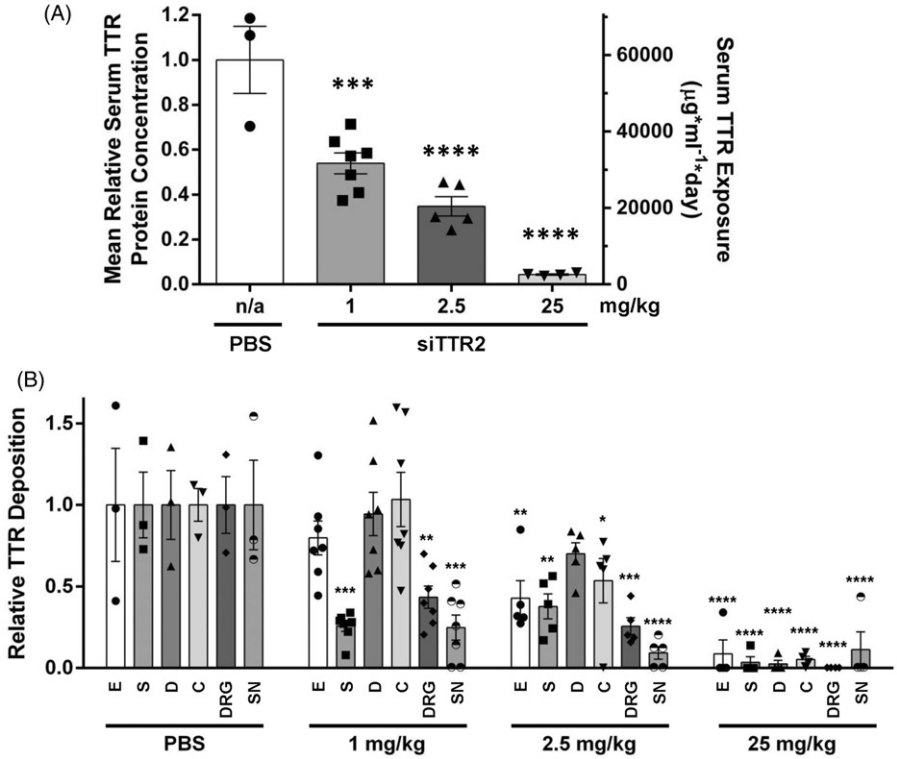

Figure 4. TTR tissue deposit regression correlates with RNAi-mediated knockdown of TTR. TTR tissue deposition in 15-month-old hTTR V30M HSF1± mice following repeat administration of PBS or siTTR2. (A) Mean relative serum TTR protein concentration (left y-axis) and total serum TTR protein exposure (right y-axis) during the 12-week course of treatment with PBS or siTTR2 at 1, 2.5 or 25 mg/kg. Each symbol represents the time averaged mean serum TTR protein concentration for each respective mouse, relative to PBS treated animals. The bar represents the group mean relative serum TTR protein concentration at a given dose level; error bars represent SEM. The treatment effect determined using 1-way ANOVA with Bonferroni's multiple comparison test. (B) Relative TTR tissue deposition in: E, esophagus; S, stomach; D, duodenum; C, colon; SN, sciatic nerve; DRG, dorsal root ganglion. Bar height represents group mean relative deposition; error bar represents the SEM; individual data point for each animal displayed as symbols within the bar. The treatment effect determined using 2-way ANOVA with Bonferroni's multiple comparison test. Group size: PBS, $n=3$; 1 mg/kg, $n=7$; 2.5 mg/kg, $n=5$, 25 mg/kg, $n=4$. Statistical analyzes: $^{*}p<0.05$, $^{**}p<0.01$, $^{***}p<0.001$, $^{****}p<0.0001$.

deposits in peripheral tissues known to be sites of pathological TTR deposition in ATTR Val30Met patients.

The extent of TTR knockdown correlates with TTR deposit regression

Protein aggregation is a concentration dependent phenomenon and studies in other amyloidoses indicate that therapeutic benefit is correlated with the extent of reduction in circulating levels of the corresponding pathogenic protein [54,55]. In most cases of ATTR amyloidosis, the pathogenic protein arises directly from circulating TTR [47] and as such reduced exposure to circulating TTR should also reduce exposure to the pathogenic protein. To evaluate the extent of reduction in TTR exposure required for therapeutic benefit, siTTR2 was administered to 15-month-old hTTR V30M HSF1± mice at different dose levels to generate varying degrees of TTR knockdown. Animals received weekly subcutaneous injections of siTTR2 at 1, 2.5 or 25 mg/kg for a total of 12 weeks; interim serum samples were collected to evaluate relative protein knockdown and serum TTR protein exposure during the course of the experiment. TTR tissue deposition was evaluated 2 days after the 12th and final dose.

The baseline serum TTR concentration varied from animal to animal (data not shown) and, given the range of knockdown observed in the study, a broad range of serum TTR exposure was achieved, thus allowing the evaluation of its impact on TTR deposition (Figure 4A). As mentioned earlier, administration of siTTR2 at 25 mg/kg resulted in >95% knockdown of serum TTR (Figure 4A). Further, repeat administration at 25 mg/kg resulted in statistically significant reduction of TTR deposition in the esophagus, stomach, duodenum, colon, sciatic nerve and dorsal root ganglion (Figure 4B). In contrast, weekly administration at 1 and 2.5 mg/kg resulted in a lower and more variable reduction in average serum TTR concentration (47% and 66%, respectively; Figure 4A). Similarly, less TTR deposit reduction was also observed across the sites of TTR deposition evaluated (Figure 4B). Although TTR deposit reduction was not statistically significant across all tissues and doses examined, a clear trend emerged in which it appeared that intermediate gene silencing led to intermediate levels of TTR deposit reduction. To better quantify this effect, the relative extent of TTR tissue deposition in each animal was plotted against the respective serum TTR exposure for each tissue (Supplementary Figure 1). Although the precise mechanism of TTR tissue deposition is unknown, these data suggest that the extent of TTR tissue deposit regression, to a first approximation, was linearly correlated with reductions of serum TTR protein exposure. Taken together, these data suggest that while complete knockdown of serum TTR levels is likely most efficacious, intermediate levels of serum TTR protein knockdown can lead to significant and meaningful reduction in TTR tissue deposition.

TTR knockdown more effective than tetramer stabilization in mouse model of h-ATTR amyloidosis

To compare the effect of RNAi-mediated TTR silencing versus tetramer stabilization on existing deposits, 15-month-old hTTR V30M HSF1± mice were administered the tetramer stabilizer tafamidis (0.8 mg fixed dose) or its respective control (meglumine). The formulations were administered via subcutaneous injection 3 times per week for 6 weeks (see methods). To confirm successful administration of tafamidis, serum TTR tetramer stability was evaluated on days -7, 9, 23, 37 and 52. TTR protein tissue deposition was evaluated on day 52.

Subcutaneous injections of tafamidis resulted in >100% stabilization of serum TTR, the magnitude of which was equivalent to or greater than that observed in clinical trials (Supplementary Figure 2A and B; Figure 5A) [48]. At this level of stabilization, only the sciatic nerve and dorsal root ganglion exhibited a decrease in average TTR tissue deposition (~64% and 42%, respectively); TTR deposit regression was not observed in other tissues (Figure 5B). Although not statistically significant, the reductions suggest the TTR stabilizer is modulating TTR deposition to some extent in this model and are consistent with previously observed clinical efficacy [28]. The design and duration of this experiment was comparable to that described earlier for siTTR1 and thus allows for comparison of these two modalities (Figure 3). In contrast to tafamidis, siTTR1 demonstrated robust and significant TTR tissue deposition reductions in the sciatic nerve and dorsal root ganglion (72% and 81%, respectively). Further, siTTR1 resulted in robust and significant reductions in TTR deposition in all other tissues evaluated except the stomach, suggesting that RNAi-mediated TTR knockdown may be a more effective approach to reduce overall TTR tissue deposit burden (Figure 3C).

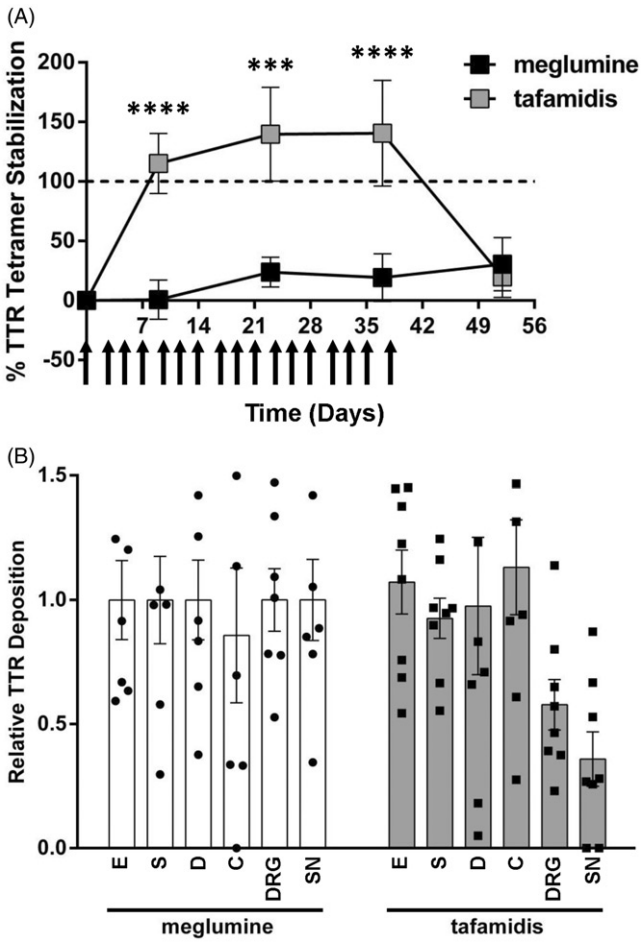

Figure 5. Effect of tetramer stabilization on TTR tissue deposition. TTR tissue deposition in 15-month-old hTTR V30M HSF1$^{\pm}$ mice following repeat administration of tafamidis or meglumine control. (A) Extent of serum TTR tetramer stabilization by tafamidis. Data represent mean % TTR tetramer stabilization at each time point (meglumine control, $n = 4$; tafamidis, $n = 8$); error bars represent SEM. Dashed horizontal line indicates 100% stabilization (2× initial tetramer concentration). Arrows indicate administration of tafamidis or meglumine control. See Supplementary Figure 2 for more detail. (B) Relative TTR tissue deposition in: E, esophagus; S, stomach; D, duodenum; C, colon; DRG, dorsal root ganglion; SN, sciatic nerve. Treatment effect in (A) and (B) evaluated using 2-way ANOVA with Bonferroni's multiple comparison test (***$p < 0.001$, ****$p < 0.0001$).

Systemic administration of RNAi therapeutic candidates mediate robust and durable knockdown of serum TTR in non-human primates (NHP)

ATTR amyloidosis is a progressive and debilitating disease that, although somewhat heterogeneous, will likely require life-long treatment to mitigate the deleterious effects of TTR protein misfolding. The cynomolgus monkey (*Macaca fascicularis*) is a species that has shown pharmacologic responses to siRNAs and is commonly used for non-clinical pharmacodynamic evaluations to aid in the prediction of human translation. To better understand the pharmacodynamic properties associated with prolonged treatment, repeat administration of the investigational RNAi therapeutics patisiran and revusiran were evaluated in the cynomolgus monkey.

Patisiran is an intravenously (IV) administered siRNA lipid nanoparticle formulation targeting TTR that is currently in clinical development for the treatment of hereditary ATTR amyloidosis with polyneuropathy [36]. To evaluate the effect of repeat administration, patisiran was administered at 0.3 mg/kg every 4 weeks for a total of seven doses (Figure 6A, Group 1). Approximately 85% knockdown of serum TTR was observed following the initial dose. Serum TTR levels returned to ~50% of baseline prior to administration of the second dose 4 weeks later. The extent of maximal knockdown increased to ~96% with repeat administration. To further explore the impact of dose frequency on knockdown, four animals were dosed at 0.3 mg/kg every 4 weeks and then switched to a once every 3-week paradigm starting at week 15 for an additional four doses (Figure 6A, Group 2). Although more frequent dosing of patisiran resulted in similar degrees of maximal TTR knockdown (96% versus 97%, Group 1 versus Group 2, respectively), the more frequent dosing regimen employed in Group 2 more effectively blunted the extent of recovery toward baseline prior to administration of the subsequent dose (70% versus 85% knockdown, Group 1 versus Group 2, respectively). Ultimately, this led to greater overall reduction in serum TTR exposure as average TTR knockdown between week 15 and 25 was 84% versus 92% (Group 1 versus Group 2, respectively).

Revusiran is a subcutaneously administered GalNAc-siRNA conjugate targeting TTR currently in clinical development for the treatment of hereditary ATTR amyloidosis with cardiomyopathy (NCT02319005). To evaluate the pharmacology of revusiran, NHPs were administered PBS or revusiran subcutaneously at three dose levels (2.5, 5 and 10 mg/kg) for a total of nine doses; five daily doses in week 1, followed by weekly dosing for 4 weeks. Daily dosing during week 1, which enables more rapid TTR lowering, followed by weekly dosing, which is sufficient to maintain TTR lowering, is the dosing paradigm currently being evaluated in Phase 3 clinical trials. At 10 mg/kg, up to 95% knockdown, relative to pre-dose TTR levels, was observed within 14–18 days of the first dose (Figure 6B). As expected, no reduction in serum

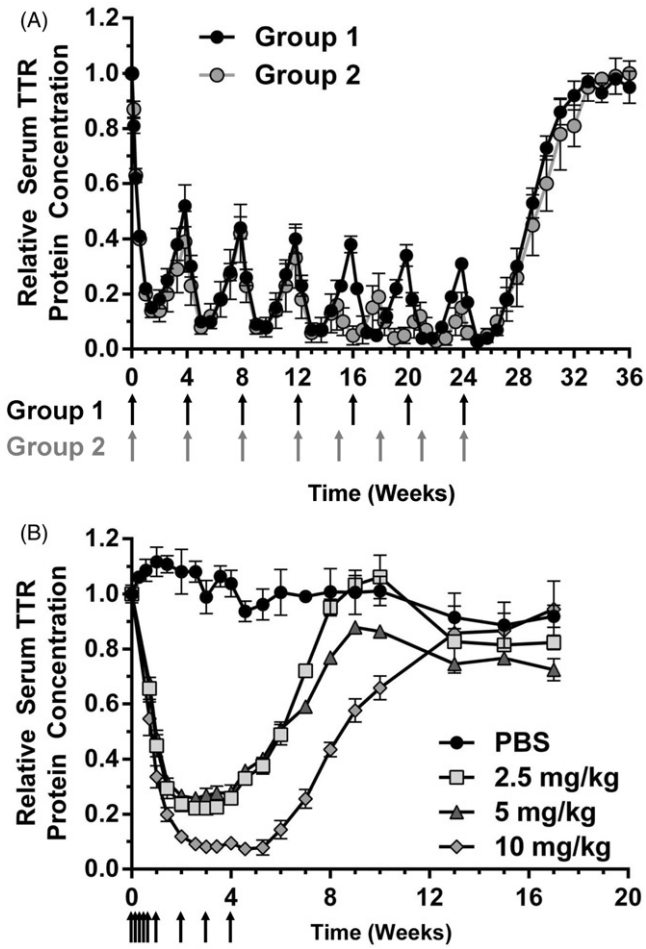

Figure 6. RNAi-mediated knockdown of TTR following repeat administration of patisiran and revusiran in the cynomolgus monkey. (A) Patisiran was administered to cynomolgus monkeys ($n = 4$ per group, 2 males, 2 females) at 0.3 mg/kg once every 4 weeks for seven total doses (Group 1) or once every 4 weeks (four doses) followed by once every 3 weeks (four doses) for a total of eight doses (Group 2). Note: An incomplete data set from Group 1 was previously published [36] (B) Revusiran was administered to cynomolgus monkeys using 5 daily doses in week 1 (D0, D1, D2, D3 and D4) followed by weekly dosing for 4 weeks (D7, D14, D21 and D28) at dose levels of 2.5, 5 or 10 mg/kg. $N = 3$ per group. For both experiments, mean relative serum TTR protein concentration was measured and calculated as described earlier; error bars represent SEM. Arrows indicate time of dosing.

TTR protein was observed in the PBS control group. Knockdown of TTR was durable with recovery to within 80–90% of baseline between 63- and 91-day post-cessation of dosing in all dose cohorts. At the top dose of 10 mg/kg, maximal serum TTR knockdown was maintained for almost 2 weeks following the final dose and suggests a once weekly dosing paradigm is more than sufficient to maintain robust, steady serum TTR knockdown.

Discussion

siRNA formulations targeting TTR resulted in robust knockdown of hepatic TTR mRNA and serum protein in hTTR V30M HSF1$^{\pm}$ transgenic mice. Further, RNAi-mediated knockdown of hepatic TTR inhibited TTR protein deposition and promoted the regression of existing TTR deposits in pathologically relevant tissues. Finally, the extent of regression of TTR tissue deposits correlated with the extent of reduction in serum TTR exposure. Together, these data suggest that RNAi-mediated knockdown of hepatic TTR expression, by virtue of significantly reducing the systemic concentration of the precursor to the protein aggregate, can prevent the formation of new deposits and thereby allow an otherwise overwhelmed endogenous repair process to reverse the consequences of protein misfolding. Further, while maximal protein knockdown would be ideal, the data suggests that lower levels of knockdown also have potential to result in clinical benefit. It should be noted that the RNAi formulations evaluated in this study only modulate TTR gene expression in hepatocytes and may be limited to treating only those manifestations associated with hepatocyte-derived TTR. Silencing extra-hepatic TTR gene expression in clinically important tissues such as the retinal pigmentosa epithelium and choroid plexus will likely require different siRNA delivery solutions. Also, it should be noted that the hTTR V30M HSF1$^{\pm}$ mouse model does not exhibit neurological complications and other advanced manifestations of ATTR Val30Met. However, the model does seem to recapitulate the initial steps of TTR aggregation and tissue deposition and is therefore valuable for evaluating this hypothesis. For example, in early stage ATTR Val30Met patients, analysis of sural nerve biopsies indicate that non-fibrillar TTR deposits appear in tissues of patients prior to fibrillar TTR deposition, suggesting the non-fibrillar to fibrillar structural transition may be an important step in early disease progression [56]. Similarly, while most TTR protein deposits observed in hTTR V30M HSF1$^{\pm}$ transgenic mice are non-fibrillar in nature, fibrillar deposits have been detected in the stomach and sciatic nerve with varying degrees of phenotypic penetrance and suggest this model may reproduce the salient features of this early structural transition [46]. In addition, the specific tissues exhibiting TTR protein deposition in hTTR V30M HSF1$^{\pm}$ transgenic mice are similar to that observed in ATTR Val30Met patients, suggesting the spatial pattern of deposition is also preserved. At present, it is unclear to what extent the mouse model recapitulates deposit load in each tissue as well as deposit assembly dynamics. However, given structural and spatial aspects of TTR deposition appear preserved, it suggests these mice may mimic early stage ATTR Val30Met. Consistent with these results, data from an ongoing Phase 2 open-label clinical trial with the investigational RNAi therapeutic patisiran demonstrated sustained TTR suppression and evidence of potential halting of disease progression in patients with hereditary ATTR with polyneuropathy [57]. Although preliminary, the data provide further support for the TTR lowering therapeutic hypothesis and the predictions made by this mouse model.

To compare the efficacy of the tetramer stabilization approach to that of RNAi-mediated TTR knockdown, we evaluated tafamidis in the hTTR V30M HSF1$^{\pm}$ model and quantified the impact of TTR tetramer stabilization on the regression of preexisting TTR deposits. To compensate for differences in dose frequency and route of administration, mice were administered excess tafamidis (>100× on mg/kg basis) to enable sufficient TTR tetramer stabilization. Although administration of tafamidis resulted in a significant and clinically relevant degree of serum TTR tetramer stabilization [48], only moderate TTR deposit regression

was observed in the sciatic nerve and dorsal root ganglion; consistent regression was not observed in other tissues examined. It should be noted that the study duration was chosen to allow a more direct comparison with siTTR1 (Figure 3) and, as such, it is possible that longer term administration of tafamidis may have resulted in greater deposit regression in the hTTR V30M HSF1$^{\pm}$ model. However, in these conditions, TTR lowering seems to be more effective.

Similar to studies in hTTR V30M HSF1$^{\pm}$ transgenic mice, administration of the siRNA formulations patisiran and revusiran resulted in robust and durable knockdown of TTR in non-human primates. Patisiran and revusiran are currently being evaluated in clinical trials for the treatment of hereditary ATTR amyloidosis with polyneuropathy and cardiomyopathy, respectively. Short-term pharmacodynamic (PD) effects of patisiran and revusiran were very similar to those observed in the NHP studies presented herein [36,43], suggesting that the NHP is a good model for evaluating human translation of RNAi-based therapeutics. Although further clinical validation is required, the PD effects observed in the multi-dose studies described earlier suggest robust, long-term knockdown of serum TTR here are anticipated to translate into very similar PD effects in the clinic. Given this, and the observation that siRNAs equally silence wt and mutant TTR variants, the data suggests these formulations could be broadly applicable to all patients with ATTR amyloidosis.

Conclusion

ATTR amyloidosis is a systemic, progressive, debilitating and ultimately fatal disease affecting tens of thousands of individuals worldwide. Despite the observed heterogeneity in clinical presentation, all ATTR amyloidosis arises from TTR protein misfolding and subsequent amyloid fibril deposition. RNAi therapeutics, which seek to exploit the endogenous RNAi mechanism, are an emerging class of drugs with the potential to treat an array of diseases. The data presented in this report suggest that RNAi-mediated knockdown of TTR may effectively prevent, and potentially reverse, TTR tissue deposition resulting from hepatic TTR expression and therefore represents a very promising experimental therapeutic approach for the treatment of ATTR amyloidosis.

Acknowledgements

We thank the Alnylam Formulations and Chemistry groups for providing siRNA formulations. We thank John Vest and Pritesh Gandhi for feedback.

Declaration of interest

J.S.B., A.C., S.F., J.L.S.W., S.M., D.F., J.Q., B.R.B., K.G.R., M.M., K.F., R.E.M., S.V.N. and T.S.Z. are employees and shareholders of Alnylam Pharmaceuticals Inc.

References

1. Blake CC, Swan ID, Rerat C, Berthou J, Laurent A, Rerat B. An X-ray study of the subunit structure of prealbumin. J Mol Biol 1971;61:217–24.
2. Holmgren G, Steen L, Ekstedt J, Groth CG, Ericzon BG, Eriksson S, Andersen O, et al. Biochemical effect of liver transplantation in two Swedish patients with familial amyloidotic polyneuropathy (fap-met30). Clin Genet 1991;40:242–6.
3. Kanda Y, Goodman DS, Canfield RE, Morgan FJ. The amino acid sequence of human plasma prealbumin. J Biol Chem 1974;249: 6796–805.
4. Kanai M, Raz A, Goodman DS. Retinol-binding protein: the transport protein for vitamin a in human plasma. J Clin Invest 1968; 47:2025–44.
5. Nilsson SF, Rask L, Peterson PA. Studies on thyroid hormone-binding proteins. II. Binding of thyroid hormones, retinol-binding protein, and fluorescent probes to prealbumin and effects of thyroxine on prealbumin subunit self association. J Biol Chem 1975;250:8554–63.
6. Wojtczak A, Cody V, Luft JR, Pangborn W. Structures of human transthyretin complexed with thyroxine at 2.0 a resolution and 3′,5′-dinitro-n-acetyl-l-thyronine at 2.2 a resolution. Acta Crystallogr D Biol Crystallogr 1996;52:758–65.
7. Sekijima Y, Wiseman RL, Matteson J, Hammarstrom P, Miller SR, Sawkar AR, Balch WE, et al. The biological and chemical basis for tissue-selective amyloid disease. Cell 2005;121:73–85.
8. Colon W, Kelly JW. Partial denaturation of transthyretin is sufficient for amyloid fibril formation in vitro. Biochemistry 1992;31:8654–60.
9. Lai Z, Colon W, Kelly JW. The acid-mediated denaturation pathway of transthyretin yields a conformational intermediate that can self-assemble into amyloid. Biochemistry 1996;35:6470–82.
10. Hammarstrom P, Jiang X, Hurshman AR, Powers ET, Kelly JW. Sequence-dependent denaturation energetics: a major determinant in amyloid disease diversity. Proc Natl Acad Sci USA 2002; 99(Suppl):16427–32.
11. Marcoux J, Mangione PP, Porcari R, Degiacomi MT, Verona G, Taylor GW, Giorgetti S, et al. A novel mechano-enzymatic cleavage mechanism underlies transthyretin amyloidogenesis. EMBO Mol Med 2015;7:1337–49.
12. Costa PP, Figueira AS, Bravo FR. Amyloid fibril protein related to prealbumin in familial amyloidotic polyneuropathy. Proc Natl Acad Sci USA 1978;75:4499–503.
13. Cornwell 3rd GG,, Westermark P, Natvig JB, Murdoch W. Senile cardiac amyloid: evidence that fibrils contain a protein immunologically related to prealbumin. Immunology 1981;44:447–52.
14. Wallace MR, Dwulet FE, Conneally PM, Benson MD. Biochemical and molecular genetic characterization of a new variant prealbumin associated with hereditary amyloidosis. J Clin Invest 1986;78:6–12.
15. Sipe JD, Benson MD, Buxbaum JN, Ikeda S, Merlini G, Saraiva MJ, Westermark P. Nomenclature 2014: amyloid fibril proteins and clinical classification of the amyloidosis. Amyloid 2014;21:221–4.
16. Adams D, Lozeron P, Lacroix C. Amyloid neuropathies. Curr Opin Neurol 2012;25:564–72.
17. Ando Y, Ueda M. Diagnosis and therapeutic approaches to transthyretin amyloidosis. Curr Med Chem 2012;19:2312–23.
18. Ruberg FL, Berk JL. Transthyretin (ttr) cardiac amyloidosis. Circulation 2012;126:1286–300.
19. Sekijima Y. Transthyretin (attr) amyloidosis: clinical spectrum, molecular pathogenesis and disease-modifying treatments. Transthyretin (attr) amyloidosis: clinical spectrum, molecular pathogenesis and disease-modifying treatments 2015;86:1036–43.
20. Connors LH, Lim A, Prokaeva T, Roskens VA, Costello CE. Tabulation of human transthyretin (ttr) variants, 2003. Amyloid 2003;10:160–84.
21. Cornwell GG 3rd, Sletten K, Johansson B, Westermark P. Evidence that the amyloid fibril protein in senile systemic amyloidosis is derived from normal prealbumin. Biochem Biophys Res Commun 1988;154:648–53.
22. Benson MD. Liver transplantation and transthyretin amyloidosis. Muscle Nerve 2013;47:157–62.
23. Ericzon BG, Wilczek HE, Larsson M, Wijayatunga P, Stangou A, Pena JR, Furtado E, et al. Liver transplantation for hereditary transthyretin amyloidosis: after 20 years still the best therapeutic alternative? Transplantation 2015;99:1847–54.
24. Liepnieks JJ, Benson MD. Progression of cardiac amyloid deposition in hereditary transthyretin amyloidosis patients after liver transplantation. Amyloid 2007;14:277–82.

25. Johnson SM, Connelly S, Fearns C, Powers ET, Kelly JW. The transthyretin amyloidoses: from delineating the molecular mechanism of aggregation linked to pathology to a regulatory-agency-approved drug. J Mol Biol 2012;421:185–203.
26. Coelho T, Chorão R, Sousa A, Alves I, Torres MF, Saraiva MJM. Compound heterozygotes of transthyretin met30 and transthyretin met119 are protected from the devastating effects of familial amyloid polyneuropathy. Neuromuscul Disord 1996;6:S20.
27. Longo Alves I, Hays MT, Saraiva MJ. Comparative stability and clearance of [met30]transthyretin and [met119]transthyretin. Eur J Biochem 1997;249:662–8.
28. Coelho T, Maia LF, Martins Da Silva A, Waddington Cruz M, Plante-Bordeneuve V, Lozeron P, Suhr OB, et al. Tafamidis for transthyretin familial amyloid polyneuropathy: a randomized, controlled trial. Neurology 2012;79:785–92.
29. Berk JL, Suhr OB, Obici L, Sekijima Y, Zeldenrust SR, Yamashita T, Heneghan MA, et al. Repurposing diflunisal for familial amyloid polyneuropathy: a randomized clinical trial. Jama 2013;310: 2658–67.
30. Hammarstrom P, Schneider F, Kelly JW. Trans-suppression of misfolding in an amyloid disease. Science 2001;293:2459–62.
31. Elbashir SM, Harborth J, Lendeckel W, Yalcin A, Weber K, Tuschl T. Duplexes of 21-nucleotide RNAs mediate RNA interference in cultured mammalian cells. Nature 2001;411:494–8.
32. Fire A, Xu S, Montgomery MK, Kostas SA, Driver SE, Mello CC. Potent and specific genetic interference by double-stranded RNA in caenorhabditis elegans. Nature 1998;391:806–11.
33. Sehgal A, Vaishnaw A, Fitzgerald K. Liver as a target for oligonucleotide therapeutics. J Hepatol 2013;59:1354–9.
34. Vaishnaw AK, Gollob J, Gamba-Vitalo C, Hutabarat R, Sah D, Meyers R, De Fougerolles T, et al. A status report on rnai therapeutics. Silence 2010;1:14.
35. Nair JK, Willoughby JL, Chan A, Charisse K, Alam MR, Wang Q, Hoekstra M, et al. Multivalent n-acetylgalactosamine-conjugated sirna localizes in hepatocytes and elicits robust rnai-mediated gene silencing. J Am Chem Soc 2014;136:16958–61.
36. Coelho T, Adams D, Silva A, Lozeron P, Hawkins PN, Mant T, Perez J, et al. Safety and efficacy of rnai therapy for transthyretin amyloidosis. N Engl J Med 2013;369:819–29.
37. Fitzgerald K, Frank-Kamenetsky M, Shulga-Morskaya S, Liebow A, Bettencourt BR, Sutherland JE, Hutabarat RM, et al. Effect of an rna interference drug on the synthesis of proprotein convertase subtilisin/kexin type 9 (pcsk9) and the concentration of serum ldl cholesterol in healthy volunteers: a randomised, single-blind, placebo-controlled, phase 1 trial. Lancet 2014;383:60–8.
38. Akinc A, Querbes W, De S, Qin J, Frank-Kamenetsky M, Jayaprakash KN, Jayaraman M, et al. Targeted delivery of rnai therapeutics with endogenous and exogenous ligand-based mechanisms. Mol Ther 2010;18:1357–64.
39. Jayaraman M, Ansell SM, Mui BL, Tam YK, Chen J, Du X, Butler D, et al. Maximizing the potency of sirna lipid nanoparticles for hepatic gene silencing in vivo. Angew Chem Int Ed Engl 2012;51: 8529–33.
40. Hayashi Y, Mori Y, Yamashita S, Motoyama K, Higashi T, Jono H, Ando Y, et al. Potential use of lactosylated dendrimer (g3)/alpha-cyclodextrin conjugates as hepatocyte-specific sirna carriers for the treatment of familial amyloidotic polyneuropathy. Mol Pharm 2012; 9:1645–53.
41. Akinc A, Goldberg M, Qin J, Dorkin JR, Gamba-Vitalo C, Maier M, Jayaprakash KN, et al. Development of lipidoid-sirna formulations for systemic delivery to the liver. Mol Ther 2009;17:872–9.
42. Semple SC, Akinc A, Chen J, Sandhu AP, Mui BL, Cho CK, Sah DW, et al. Rational design of cationic lipids for sirna delivery. Nat Biotechnol 2010;28:172–6.
43. Hawkins PN, Ando Y, Dispenzeri A, Gonzalez-Duarte A, Adams D, Suhr O. Evolving landscape in the management of transthyretin amyloidosis Ann Med 2015;47:625–38.
44. Sehgal A, Barros S, Ivanciu L, Cooley B, Qin J, Racie T, Hettinger J, et al. An rnai therapeutic targeting antithrombin to rebalance the coagulation system and promote hemostasis in hemophilia. Nat Med 2015;21:492–7.
45. Mui BL, Tam YK, Jayaraman M, Ansell SM, Du X, Tam YY, Lin PJ, et al. Influence of polyethylene glycol lipid desorption rates on pharmacokinetics and pharmacodynamics of sirna lipid nanoparticles. Mol Ther Nucleic Acids 2013;2:e139.
46. Santos SD, Fernandes R, Saraiva MJ. The heat shock response modulates transthyretin deposition in the peripheral and autonomic nervous systems. Neurobiol Aging 2010;31:280–9.
47. Bulawa CE, Connelly S, Devit M, Wang L, Weigel C, Fleming JA, Packman J, et al. Tafamidis, a potent and selective transthyretin kinetic stabilizer that inhibits the amyloid cascade. Proc Natl Acad Sci USA 2012;109:9629–34.
48. European medical agency assesment report, procedure no. Emea/h/c/002294. European Medical Agency 2011. Report No.: EMEA/H/C/002294.
49. Tagoe CE, Reixach N, Friske L, Mustra D, French D, Gallo G, Buxbaum JN. In vivo stabilization of mutant human transthyretin in transgenic mice. Amyloid 2007;14:227–36.
50. Xiao X, Zuo X, Davis AA, Mcmillan DR, Curry BB, Richardson JA, Benjamin IJ. Hsf1 is required for extra-embryonic development, postnatal growth and protection during inflammatory responses in mice. EMBO J 1999;18:5943–52.
51. Cavallaro T, Martone RL, Dwork AJ, Schon EA, Herbert J. The retinal pigment epithelium is the unique site of transthyretin synthesis in the rat eye. Invest Ophthalmol Vis Sci 1990;31: 497–501.
52. Harms PJ, Tu GF, Richardson SJ, Aldred AR, Jaworowski A, Schreiber G. Transthyretin (prealbumin) gene expression in choroid plexus is strongly conserved during evolution of vertebrates. Comp Biochem Physiol B 1991;99:239–49.
53. Westermark GT, Westermark P. Transthyretin and amyloid in the islets of langerhans in type-2 diabetes. Exp Diabetes Res 2008; 2008:429274.
54. Gillmore JD, Lovat LB, Persey MR, Pepys MB, Hawkins PN. Amyloid load and clinical outcome in aa amyloidosis in relation to circulating concentration of serum amyloid a protein. Lancet 2001; 358:24–9.
55. Lachmann HJ, Gallimore R, Gillmore JD, Carr-Smith HD, Bradwell AR, Pepys MB, Hawkins PN. Outcome in systemic al amyloidosis in relation to changes in concentration of circulating free immunoglobulin light chains following chemotherapy. Br J Haematol 2003;122:78–84.
56. Sousa MM, Cardoso I, Fernandes R, Guimaraes A, Saraiva MJ. Deposition of transthyretin in early stages of familial amyloidotic polyneuropathy: evidence for toxicity of nonfibrillar aggregates. Am J Pathol 2001;159:1993–2000.
57. Coelho T, Suhr O, Conceicao I, Cruz MW, Schmidt H, Juan B, Campistol J, et al. Phase 2 Open-label Extension Study of Patisiran, an Investigational RNAi Therapeutic for the Treatment of Familial Amyloid Polyneuropathy. Poster session presented at: S9 General Neurology: Neurological Treatments and Therapeutics. 67th AAN Annual Meeting; 2016 April 1825; Washington, DC.

Supplementary material available online